^{68}Ga-Pentixafor PET/CT Imaging of Chemokine Receptor CXCR4 in Chronic Infection of the Bone: First Insights

Caroline Bouter[1], Birgit Meller[1], Carsten O. Sahlmann[1], Wieland Staab[2], Hans J. Wester[3], Saskia Kropf[4], and Johannes Meller[1]

[1]Department of Nuclear Medicine, Georg-August-University Göttingen, Göttingen, Germany; [2]Department of Radiology, Georg-August-University Göttingen, Göttingen, Germany; [3]Pharmaceutical Radiochemistry, Technical University of Munich, Garching, Germany; and [4]SCINTOMICS GmbH, Fuerstenfeldbruck, Germany

Because of its role in infection and inflammatory processes, the chemokine receptor CXCR4 might be a potent target in imaging of infectious and inflammatory diseases. The aim of this pilot study was to determine whether the CXCR4 ligand ^{68}Ga-pentixafor is suitable for imaging chronic infection of the bone. **Methods:** The study comprised 14 patients with suspected infection of the skeleton who underwent ^{68}Ga-pentixafor PET/CT between April 2015 and February 2017 in our facility. ^{68}Ga-pentixafor PET/CT results were retrospectively evaluated against a histologic, bacteriologic, and clinical standard. The results were also compared with available bone scintigraphy, white blood cell scintigraphy, and ^{18}F-FDG PET/CT results. **Results:** ^{68}Ga-pentixafor PET/CT was positive in 9 of 14 patients. Diagnoses included osteitis or osteomyelitis of peripheral bone, osteomyelitis of the maxilla, and infected endoprostheses. Target-to-background ratios were 5.1–15 (mean, 8.7). Eight of 9 cases were true-positive as confirmed by pathology, bacteriology, or clinical observation. All negative cases were confirmed as true-negative by other imaging modalities and follow-up. **Conclusion:** Imaging of CXCR4 expression with ^{68}Ga-pentixafor PET/CT appears suitable for diagnosing chronic infection of the skeleton. The findings of this study reveal a possible diagnostic gain in suspected chronic infections that are difficult to diagnose by other imaging modalities.

Key Words: osteomyelitis; PET/CT; pentixafor; CXCR4; molecular imaging

J Nucl Med 2018; 59:320–326
DOI: 10.2967/jnumed.117.193854

Diagnosis of skeletal infections presents a clinical and diagnostic challenge because patients present with a variety of clinical symptoms. The diagnostic workup usually includes a combination of clinical, laboratory, and imaging findings. Whereas acute posttraumatic infections (first 2 wk after trauma or surgery) are usually diagnosed by clinical examination, common signs of infection might be absent in later phases and additional diagnostics are crucial (*1*). In acute osteomyelitis, the innate immune response, mainly including neutrophils and macrophages, is essential. Chronic osteomyelitis shows a more heterogeneous distribution of leukocytes in which components of the adaptive immune response are leading. Even though neutrophils can still play a role in chronic phases, they can be absent in some situations and lymphocytes might become the major fraction of immune cells (*2*). Because of its role in inflammatory processes and its high expression levels on lymphocytes, the chemokine receptor CXCR4 might be a potent target in imaging chronic infectious diseases. Various tumor cells overexpress CXCR4, and the radiolabeled CXCR4 ligand ^{68}Ga-pentixafor, developed in 2011, has been shown useful in imaging multiple myelomas, gliomas, and small cell lung cancer (*3–10*).

The aim of this proof-of-principle study was to determine whether ^{68}Ga-pentixafor PET/CT is a suitable method for imaging chronic infectious diseases of the skeleton.

MATERIALS AND METHODS

Patients

In total, 27 consecutive patients who underwent ^{68}Ga-pentixafor PET/CT in our facility between April 2015 and February 2017 were evaluated retrospectively. Thirteen patients were excluded, as the clinical question was carcinoma or large-vessel vasculitis and did not include infection of the bone. Therefore, the study comprised 14 consecutive patients (7 women and 7 men aged 19–78 y; mean age, 57 y) with suspected osteomyelitis. The suspected diagnosis was decided by clinical or laboratory results in the department of orthopedics or oral and maxillofacial surgery, and imaging of infection of the bone was requested. Patients came to our department following a routine workflow in which bone scintigraphy is the first line of nuclear medicine imaging. The second step of the routine workflow includes leukocyte imaging. In each case, the use of either white blood cell (WBC) imaging or ^{68}Ga-pentixafor PET/CT was discussed with the referring colleagues, and the most suitable method was chosen.

All patients were in a postinterventional stage. The suspected diagnoses included postoperative osteitis or osteomyelitis of peripheral bone ($n = 2$), postoperative spondylitis ($n = 3$), postinterventional osteitis or osteomyelitis of maxillofacial bone ($n = 4$), and infections of endoprostheses ($n = 5$).

^{68}Ga-pentixafor PET/CT was performed 2–103 mo (mean, 20 mo) after the last surgical intervention. ^{68}Ga-pentixafor PET/CT results were evaluated by histology, bacteriology, C-reactive protein (CRP) levels, and clinical follow-up. If available, the results of bone scanning, WBC scanning, and ^{18}F-FDG PET/CT were compared with those of ^{68}Ga-pentixafor PET/CT.

All procedures involving human participants were in accordance with the ethical standards of the institutional or national research

Received Mar. 24, 2017; revision accepted Jun. 27, 2017.
For correspondence or reprints contact: Caroline Bouter, Department of Nuclear Medicine, Georg-August-University Göttingen, Robert-Koch-Strasse 40, 37075, Göttingen, Germany.
E-mail: caroline.bouter@med.uni-goettingen.de
Published online Jul. 20, 2017.

committee and with the 1964 Helsinki Declaration and its later amendments or comparable ethical standards. The institutional review board approved this retrospective study. All patients signed an informed consent form.

Radiochemistry

Radiolabeling of 16 nmol of pentixafor peptide (Scintomics) was performed with a median of 1,200 MBq (range, 600–2,000 MBq) of ^{68}GaCl3 (^{68}Ge/^{68}Ga generator; iThemba Labs) in a GRP Module (Scintomics) using the cationic purification method according to good-manufacturing-practice quality standards. Radiochemical purity was determined by thin-layer chromatography and high-performance liquid chromatography (*11,12*). The peptide amount for each patient was restricted to 8 nmol of pentixafor.

PET/CT

^{68}Ga-pentixafor PET/CT was performed on a Gemini TF16 PET/CT scanner (Philips) with a 144 × 144 matrix and a 4-mm slice thickness, using low-dose CT with a 512 × 512 matrix and a 2-mm slice thickness for attenuation correction (CT attenuation correction–Scharfetter-Gummel algorithm). The reconstruction was performed using the line-of-response time-of-flight row-action maximum-likelihood (blob ordered-subset time-of-flight) algorithm.

^{68}Ga-pentixafor PET/CT was performed on all patients 60 min after injection of 166–300 MBq (mean, 245 MBq) of ^{68}Ga-pentixafor. Additionally, 3 patients were scanned using a biphasic protocol (30 and 60 min), and 2 patients were scanned at 3 different time points (30, 60, and 90 min) to determine the optimal time point for ^{68}Ga-pentixafor PET/CT imaging. Later time points were not studied because of unfavorable count statistics.

A diagnostic CT scan of the area of interest was obtained without the use of contrast agent for all patients. A nuclear medicine physician and a radiologist separately reviewed the images. ^{68}Ga-pentixafor uptake was evaluated visually, and SUV_{max} was ascertained for semiquantitative analysis ($SUV = r(a'/w)$, where r is the activity concentration [kBq/mL] measured by the PET scanner within a region of interest, a' is the amount of injected radiolabeled ^{18}F-FDG [kBq], and w is the weight of the patient [g]). The SUV_{mean} within a standardized rectangular region (25 cm^2) was measured for contralateral peripheral bone. Furthermore, target-to-background ratios (TBRs) were calculated as a surrogate marker for lesion contrast as follows: SUV_{max} (lesion)/SUV_{mean} (background).

Interpretation of Findings

^{68}Ga-pentixafor PET/CT findings were positive if uptake stronger than in the surrounding tissue was seen outside the physiologic distribution. ^{68}Ga-pentixafor PET/CT findings were true-positive when histology, bacteriology, laboratory, or indisputable macroscopic findings in clinical follow-up confirmed the PET/CT result. False-positive findings included PET/CT with abnormal ^{68}Ga-pentixafor uptake that could not be confirmed by other imaging methods (MRI or radiography) and clinical or laboratory follow-up. True-negative findings included ^{68}Ga-pentixafor PET/CT with physiologic uptake that did not show any disease in other modalities and findings confirmed by clinical follow-up, CRP, or bacteriology. False-negative findings were defined as PET/CT with physiologic uptake that showed disease in other imaging methods or follow-up. Non–attenuation-corrected PET images were additionally reviewed, because attenuation correction might mimic increased tracer uptake in implants.

The results of bone scanning, WBC scanning, and ^{18}F-FDG PET/CT were assessed by applying the same principles and methods as used in the evaluation of ^{68}Ga-pentixafor PET/CT.

Statistical Analysis

All data are given as mean ± SE. Unpaired t tests and linear regression were used for statistical evaluation. Data were analyzed for normal distribution. The Grubbs test was used to identify statistical outliers, and one significant statistical outlier was removed ($P < 0.05$) (Supplemental Fig. 1; supplemental materials are available at http://jnm.snmjournals.org). All statistics were calculated using Microsoft Excel or Prism (GraphPad Software), version 6.0e, for Mac (Apple).

RESULTS

^{68}Ga-Pentixafor PET/CT Results

^{68}Ga-pentixafor PET/CT was positive in 9 of 14 patients, finding osteitis or osteomyelitis of the peripheral bone ($n = 3$), osteomyelitis of the maxilla or mandibula ($n = 2$), and spondylodiskitis and infected endoprostheses ($n = 4$).

SUV_{max} was 2.2–4.5 (mean, 3.3), and TBR was 5.1–15 (mean, 8.7). In 5 cases, a multiphasic protocol was used for image acquisition. In 3 of these cases, ^{68}Ga-pentixafor PET/CT was positive. TBR did not significantly differ at 30, 60, or 90 min after injection of ^{68}Ga-pentixafor.

^{68}Ga-pentixafor PET/CT results were confirmed in 8 of 9 patients with PET/CT-positive findings by pathology ($n = 3$), bacteriology ($n = 3$), and clinical follow-up ($n = 2$) and therefore was true-positive. Pathology confirmed chronic lymphocytic osteomyelitis in 3 cases. Bacteriology showed *Staphylococcus aureus* on an external fixator, on a partial knee replacement, and on a spacer from a removed knee arthroplasty. One patient showed a purulent fistula surrounding a metatarsophalangeal prosthesis on follow-up. The prosthesis was removed afterward, and the CRP values normalized postoperatively. A histologic or bacteriologic examination of the prosthesis was not performed (Fig. 1). The remaining patient showed an infected knee endoprosthesis on ^{68}Ga-pentixafor PET/CT, and CRP normalized after removal of the prosthesis.

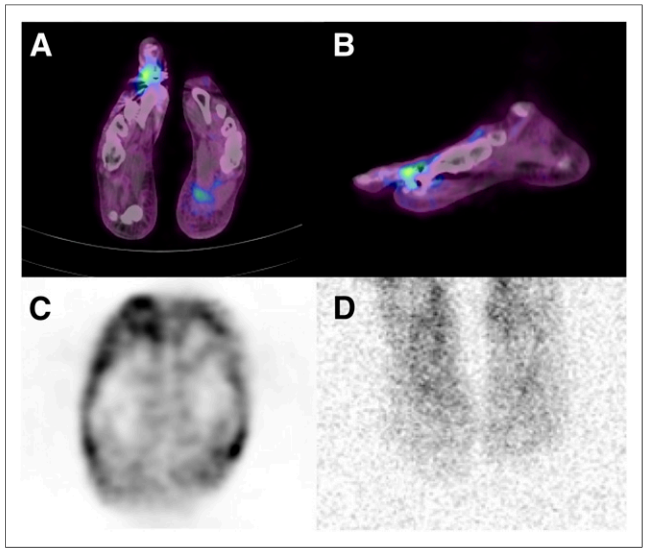

FIGURE 1. Infected metatarsophalangeal prosthesis in 43-y-old woman with elevated CRP 14 mo after intervention. (A and B) ^{68}Ga-pentixafor PET/CT shows elevated tracer uptake at infected prosthesis at right metatarsophalangeal joint I in transversal (A) and sagittal (B) views. (C) Transversal non–attenuation-corrected PET image also shows increased uptake around prosthesis, indicating that attenuation correction does not influence outcome of ^{68}Ga-pentixafor PET/CT by mimicking increased tracer uptake. (D) Planar view of ^{111}In-oxine scintigraphy 24 h after injection is negative for uptake.

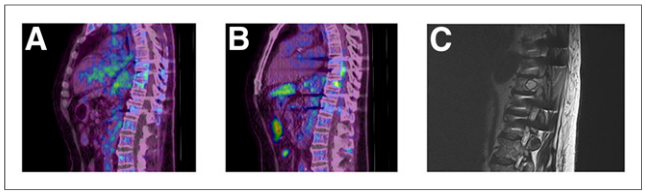

FIGURE 2. Plasmocytoma in 62-y-old man with elevated CRP and suspected spondylodiskitis. (A and B) ^{68}Ga-pentixafor (A) and ^{18}F-FDG (B) PET/CT (sagittal view) shows increased tracer uptake in multiple vertebrae, with maximum in thoracic vertebrae 10 and 11. (C) MRI shows plasmocytoma in thoracic vertebrae 10 and 11.

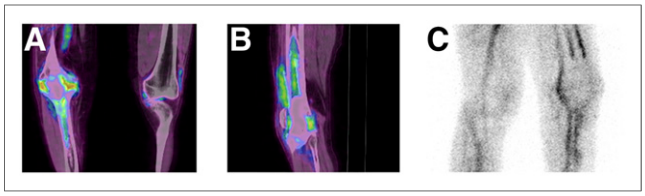

FIGURE 3. Distinct osteomyelitis in 52-y-old patient with elevated CRP 5 mo after removal of total-knee arthroplasty and implantation of spacer. (A and B) Coronal (A) and sagittal (B) ^{68}Ga-pentixafor PET/CT images show increased tracer uptake in tibia and femur, respectively, including bone marrow compartment. (C) Sagittal ^{99m}Tc-besilesomab scintigraphy image 4 h after injection shows osteitis without increased uptake in bone marrow.

One ^{68}Ga-pentixafor PET/CT–positive finding was false-positive. MRI showed a necrotic plasmacytoma in a vertebral body instead of spondylitis. This patient initially showed a positive CRP result, which persisted during follow-up (Fig. 2).

The results of ^{68}Ga-pentixafor PET and diagnostic CT were concordant in 4 of 9 cases. The remaining 5 cases were negative on CT but positive on PET.

CRP was initially positive on 6 of 8 true-positive cases, ranging between 10.7 and 167 mg/L (mean, 46.2 mg/L), and normalized in all true-positive cases during follow-up. SUV_{max} did not correlate with CRP levels ($r = 0.002$, Supplemental Fig. 1).

^{68}Ga-pentixafor PET/CT was negative in 5 of 14 patients. The PET/CT results were confirmed by follow-up with indisputable results ($n = 5$) and therefore were true-negative. The final diagnoses included broken screws in a case of spondylodesis ($n = 2$), aseptic loosening of a knee endoprosthesis ($n = 2$), and postinterventional aseptic changes of the mandible.

The results of ^{68}Ga-pentixafor PET and diagnostic CT were concordant in all 5 cases. The sensitivity of ^{68}Ga-pentixafor PET/CT was 89%, and the specificity was 83%.

Table 1 shows patient characteristics, PET/CT results, final diagnoses, and CRP for ^{68}Ga-pentixafor PET/CT–positive patients. Table 2 summarizes the results and characteristics of ^{68}Ga-pentixafor PET/CT–negative patients.

Other Nuclear Medicine Imaging Methods

Other nuclear medicine imaging methods are summarized in Table 3. Three-phase bone scintigraphy was performed on 11 of 14 patients. All scintigraphy results were positive. The results were confirmed as true-positive in 7 of 11 patients by pathology ($n = 3$) or bacteriology ($n = 4$). The remaining 4 cases were false-positive because the results were not confirmed in follow-up.

^{18}F-FDG PET/CT was performed on 4 patients. The results were true-negative in one case of suspected spondylodiskitis and positive in 2 cases of osteitis or osteomyelitis of the peripheral bone and one of spondylodiskitis. SUV_{max} was 3.2–7 (mean, 5.6), and TBR was 4.5–17.5 (mean, 10.5). There were no significant differences in TBR between ^{68}Ga-pentixafor PET/CT and ^{18}F-FDG PET/CT ($P = 0,65$). Whereas the cases of osteitis and osteomyelitis were true-positive (proven by bacteriology and pathology), the case of spondylodiskitis was false-positive, showing a necrotic plasmocytoma on MRI. The distribution pattern of ^{18}F-FDG was comparable to the pattern of pentixafor uptake except for one case, a Pilon fracture of the tibia that showed additional ^{18}F-FDG uptake around the bone canals of an external fixator (SUV_{max}, 2.2). ^{68}Ga-pentixafor PET/CT was true-negative around these bone canals.

WBC scintigraphy was performed in 7 cases (^{111}In-oxine–labeled leukocyte scintigraphy [$n = 6$] and ^{99m}Tc-besilesomab [$n = 1$]). Scintigraphy was true-positive in 2 of 7 cases as proven by bacteriology. ^{111}In-oxine scintigraphy showed an infected knee resurfacing in one case, and ^{99m}Tc-besilesomab showed osteitis after a knee spacer implantation. Both cases were also positive on ^{68}Ga-pentixafor PET/CT. However, ^{68}Ga-pentixafor PET/CT

TABLE 1
Data for Patients with True-Positive Results on ^{68}Ga-Pentixafor PET/CT

Patient no.	Sex	Age (y)	Diagnosis	Proof	SUV_{max}	TBR	CRP	CRP FU
1	M	21	Osteitis, femur	B	4.5	10.5	167	Neg
2	M	65	Osteomyelitis, tibia	P	2.2	5.5	Neg	Neg
3	M	77	Infected knee resurfacing	B	3.9	4.3	Neg	Neg
4	M	52	Osteomyelitis around knee spacer	B	3.5	7	25.4	13.9
5	M	62	Necrotic plasmacytoma	MRI, FU	3.6	7.2	10.7	12.1
6	F	43	Infected prosthesis, metatarsophalangeal	FU	2.2	5.5	15	Neg
7	F	62	Osteomyelitis, maxillary	P	3.7	7.4	Neg	Neg
8	F	51	Septic loosening, knee endoprosthesis	FU	2.9	7.3	13.3	Neg
9	F	73	Osteomyelitis, mandibular	P	3.4	7.8	47.9	neg

FU = follow-up; B = bacteriology; neg = negative; P = pathology.

TABLE 2
Data for Patients with True-Negative Results on ^{68}Ga-Pentixafor PET/CT

Patient no.	Sex	Age (y)	Proof	SUV_{max}	TBR	CRP FU
1	F	61	Spondylodesis with broken screw	FU	Neg	Neg
2	M	19	Postinterventional, mandible	FU	11.4	Neg
3	F	75	Aseptic loosening, knee endoprosthesis	FU	Neg	Neg
4	M	78	Spondylodesis with broken screw	FU	Neg	Neg
5	F	48	Postinterventional, mandible	FU	Neg	Neg

FU = follow-up; neg = negative.

revealed distinct osteomyelitis in the patients with the knee spacer implantation, as proven by bacteriology, whereas ^{99m}Tc-besilesomab showed only osteitis (Fig. 3).

In the remaining 5 of 7 cases, WBC scintigraphy (using ^{111}In-oxine–labeled leukocytes) was negative. Two of these cases were false-negative as confirmed by pathology. The remaining 2 cases were true-negative as confirmed by follow-up.

Other Non–Nuclear Medicine Imaging Methods

MRI was performed on 2 patients. In one case it showed a necrotic plasmocytoma, which was false-positive on ^{68}Ga-pentixafor PET/CT and on ^{18}F-FDG PET/CT, as described above (Fig. 2). The second case was negative on MRI, which was limited by multiple artifacts due to an external fixator. This case was true-positive on ^{68}Ga-pentixafor PET/CT, showing osteitis of the femur.

TABLE 3
Comparison of Imaging Methods

	Pentixafor							
Result	True/false?	CT	BS	FDG	Ind	Besi	MRI	Proof
Positive								
Patient 1	TP	TP	—	TP	—	—	FN	B
Patient 2	TP	FN	TP	TP	FN	—	—	P
Patient 3	TP	FN	TP	—	TP	—	—	B
Patient 4	TP	FN	TP	—	—	TP	—	B
Patient 5	FP	FP	—	FP	—	—	TP	FU
Patient 6	TP	TP	TP	—	FN	—	—	FU
Patient 7	TP	FN	TP	—	FN	—	—	P
Patient 8	TP	FN	TP	—	—	—	—	FU
Patient 9	TP	TP	TP	—	—	—	—	P
Negative								
Patient 1	TN	TN	FP	TN	—	—	—	FU
Patient 2	TN	TN	FP	—	—	—	—	FU
Patient 3	TN	TN	FP	—	TN	—	—	FU
Patient 4	TN	TN	—	—	—	—	—	FU
Patient 5	TN	TN	FP	—	TN	—	—	FU

Pentixafor = ^{68}Ga-pentixafor PET/CT; BS = 3-phase bone scintigraphy; FDG = ^{18}F-FDG PET/CT; Ind = ^{111}In-oxine–labeled leukocyte scintigraphy; Besi = ^{99m}Tc-besilesomab; TP = true-positive; FN = false-negative; FP = false-positive; TN = true-negative; B = bacteriology; P = pathology; FU = follow-up.

DISCUSSION

The data presented here show the usefulness of ^{68}Ga-pentixafor PET/CT in imaging chronic skeletal infections.

Ligand–CXCR4 interactions activate the mitogen-activated protein kinase and phosphoinositid-3 kinase signaling pathway, altering cell adhesion, migration, and homing of T and B lymphocytes, macrophages, neutrophils, and eosinophils. CXCR4 is essential for leukocyte trafficking to the site of infection (*13–16*). The only known CXCR4 ligand, CXCL12, plays a crucial role in inflammatory diseases such as rheumatoid arthritis. CXCR4 is expressed by 78%–88% of T lymphocytes in the peripheral blood and by more than 90% of postmigrational T cells (*17–19*). RNA expression levels also identified lymphocytes as the major CXCR4-expressing mature cell fraction in tissues of the immune system (*20*). Up- and downregulation of CXCR4 expression is differential on neutrophils, monocytes, and lymphocytes modulated by tumor necrosis factor–α and interferon–γ (*19,21*). Because chronic osteomyelitis can, in certain situations, include mainly lymphocytes at the site of infection, a specific tracer should be able to detect lymphocytes, and therefore CXCR4 is a promising target for imaging chronic infection of the bone (*2*).

Imaging of skeletal infection can be challenging. Radiologic imaging, mainly radiography or CT, are the first-line imaging methods in suspected skeletal infections. However, several pitfalls have to be considered. Radiography, MRI, and CT imaging are aggravated by metal implants because of the resulting artifacts, and early stages of chronic infection might be missed because sequestering or fistulas might not have been formed yet.

Several nuclear medicine imaging methods have become established for imaging suspected infection of the bone, including conventional bone scintigraphy, WBC imaging, and ^{18}F-FDG PET/CT.

Conventional bone scintigraphy is highly sensitive but has a limited specificity, as a variety of conditions besides osteomyelitis show an altered bone metabolism and positive results on bone scintigraphy (*22*). In our study, bone scintigraphy, if available, had positive results in all patients. However, bone scintigraphy was false-positive in 36% of cases. WBC imaging (labeled leukocytes and antigranulocyte antibodies) shows unfavorable low sensitivity and specificity in the axial skeleton (*23*). Even in the diagnosis

of infection in the peripheral skeleton, sensitivity and specificity are suboptimal. In a multinational, phase III clinical study in 22 European centers comparing antigranulocyte imaging with ^{99m}Tc-besilesomab and ^{99m}Tc-labeled WBCs in patients with peripheral osteomyelitis, the sensitivity of labeled WBC imaging was only 59%, and that of ^{99m}Tc-besilesomab was 75%. The specificity of labeled WBC imaging was 80% and that of ^{99m}Tc-besilesomab was 72% (*24*). Furthermore, Ivancevic et al. (*24*) displayed problems with an antigranulocyte antibody Fab′ fragment in low-grade chronic bone infections. Because neutrophil components of infection are not always present in chronic osteomyelitis, the use of labeled WBC imaging may be of limited value in some patients (*25*).

The use of hybrid imaging techniques combining metabolic information with anatomic details can improve both sensitivity and specificity, with a diagnostic gain of up to 48% compared with SPECT (*26–28*).

In a metaanalysis including a total of 163 cases, ^{18}F-FDG PET/CT was the most sensitive technique in imaging chronic osteomyelitis in the central and peripheral skeleton, with a sensitivity of 96% and a specificity of 91% (*29*). These results were confirmed by Jamar et al. (*30*), with a diagnostic accuracy of 95% in available data (a total of 287 cases). Despite these advantages, ^{18}F-FDG PET/CT shows limitations in early posttraumatic situations and in infected endoprostheses. Within the first 3 mo after surgery, the formation of granulomatous tissue complicates the diagnostics of osteomyelitis with possible false-positive results (*31*). In the literature, those patients who might cause a possible bias in the available data are rarely included. For example, Guhlmann et al. (*32*) evaluated ^{18}F-FDG PET/CT and antigranulocyte antibody scintigraphy in a prospective setting in 51 patients with suspected osteomyelitis. The study design excluded all patients who underwent bone surgery within the last 2 y. However, the study showed an excellent diagnostic accuracy for ^{18}F-FDG PET/CT in both the peripheral (95%) and the axial (93%) skeleton. Including patients within the first 3 mo of surgery might significantly lower those numbers. Endoprostheses also induce the formation of reactive granulation tissue, reducing the specificity of ^{18}F-FDG PET/CT (*33,34*). In a review of van der Bruggen et al. (*35*), sensitivity and specificity widely varied in patients with orthopedic implant infections (sensitivity, 28%–91%; specificity, 9%–97%).

Therefore, several clinical situations might profit from an additional PET/CT tracer primarily imaging lymphocytes: early posttraumatic osteomyelitis, infected endoprostheses, and osteomyelitis of the axial skeleton. These situations are challenging and require the utmost in diagnostic accuracy. In our study, patients with exactly these clinical questions, who are difficult to diagnose and normally not included in pilot studies, had true-positive results with ^{68}Ga-pentixafor PET/CT. Results were true-positive for 4 patients with infected endoprostheses, 2 patients with posttraumatic chronic peripheral osteomyelitis, and 2 patients with chronic osteomyelitis of the jaws. In this retrospective evaluation, only one patient with suspected osteomyelitis presented to our facility for ^{68}Ga-pentixafor PET/CT in the early postinterventional phase at 2 mo after surgery. This patient had true-positive results. However, the results of one patient are not enough to speculate on whether ^{68}Ga-pentixafor PET/CT might resolve this issue.

Interestingly, ^{68}Ga-pentixafor uptake was independent of CRP levels in our study, as CRP-negative cases also showed sufficient uptake. This finding might indicate an added value for pentixafor, as CRP results can be heterogeneous in chronic osteomyelitis and infection of endoprostheses. Michail et al. described a sensitivity of 85% for CRP in osteomyelitis (*36*).

^{68}Ga-pentixafor PET/CT showed high TBR comparable to that of ^{18}F-FDG. A high TBR is essential for diagnostics in nuclear medicine, helping distinguishing disease states from physiologic tracer uptake. Previous studies of various malignancies also showed high TBRs, and the first approaches toward CXCR4-directed endoradiotherapy were recently demonstrated (*37*).

One patient with suspected spondylodiskitis was false-positive for skeletal infection in our study. According to the initial clinical investigators in our facility, spondylodiskitis was suggested and CT also showed infection of 2 consecutive vertebrae in this patient. However, retrospectively, ^{68}Ga-pentixafor uptake was increased in multiple vertebrae, pointing to a hematopoietic disease. MRI showed a plasmocytoma in multiple vertebrae. The findings were ruled false-positive because increased uptake was not confirmed to represent an infection. In the pathophysiology of plasmocytomas, CXCR4 plays an essential role in recruiting malignant cells to the bone marrow, showing a strong correlation between CXCR4/CXCL12 activation and bone infiltration (*38,39*). Earlier studies also demonstrated the suitability of ^{68}Ga-pentixafor in PET/CT imaging in plasmocytoma patients, emphasizing CXCR4 as a potential target in plasmocytoma therapy (*5,37,40*).

In all patients who showed negative results on ^{68}Ga-pentixafor PET/CT, the results were true-negative, implying that a good negative predictive value can be assumed for the method. Within the group of patients with true-negative findings, even cases that are difficult to image—such as postinterventional patients or patients with endoprostheses—were diagnosed correctly, indicating that the method might be valuable in exclusion diagnostics.

^{18}F-FDG PET/CT results were comparable to ^{68}Ga-pentixafor PET/CT results in our study. The distribution pattern and TBR of ^{18}F-FDG and pentixafor were comparable within the lesions. However, in one osteomyelitis case with a Pilon fracture of the tibia, additional uptake of ^{18}F-FDG was present around the bone canals of an external fixator whereas no CXCR4 expression was detected in those areas. The case with suspected spondylodiskitis was false-positive on ^{18}F-FDG PET/CT and ^{68}Ga-pentixafor PET/CT because both CXCR4 and GLUT1 are known to be overexpressed in plasmocytomas. In this case, MRI was decisive.

Furthermore, our study displayed known issues with the diagnostic accuracy of ^{111}In-oxine-leukocyte scintigraphy in chronic osteomyelitis of the axial skeleton (*41–43*). A metaanalysis of Termaat et al. (*29*) showed that leukocyte scintigraphy of the axial skeleton was the least sensitive of the evaluated imaging methods. Several mechanisms are supposed to cause a loss of sensitivity. One is the low TBR between early neutrophil infection and bone marrow activity, and another is the presence of unspecific cold lesions, which are assumed to be caused by blood vessel compression or microthrombotic occlusion (*29*). In our study, the case of osteomyelitis of the mandible was not detected by ^{111}In-oxine leukocyte scintigraphy, but ^{68}Ga-pentixafor PET/CT was true-positive (Fig. 4). Earlier studies focusing on bone scintigraphy and WBC scintigraphy in acute and chronic osteomyelitis of the jaw showed the high sensitivity of the combination of the 2 methods in acute osteomyelitis, decreasing in chronic infections (*44,45*).

^{99m}Tc-besilesomab detected osteitis after a knee spacer implantation but to a smaller extent than shown by ^{68}Ga-pentixafor PET/CT, which distinctly revealed osteomyelitis. It is suggested that the small

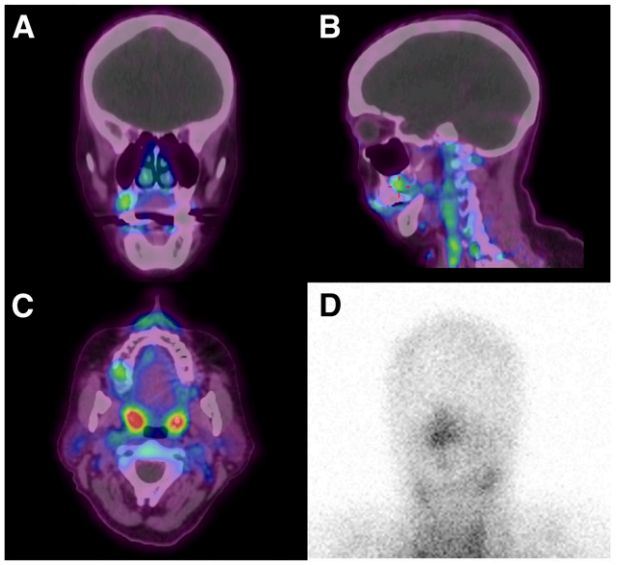

FIGURE 4. Osteomyelitis of maxilla in 62-y-old woman 3 mo after intervention. (A–C) ^{68}Ga-pentixafor PET/CT shows osteomyelitis of the maxilla on coronal (A), sagittal (B), and transversal (C) views. (D) Planar ^{111}In-oxine scintigraphy image 24 h after injection shows physiologic tracer uptake.

^{68}Ga-pentixafor molecule accumulates more effectively at the site of infection than does a complete IgG antibody, with its slow kinetics.

This study proved the principle of using ^{68}Ga-pentixafor PET/CT in chronic skeletal infections. ^{68}Ga-pentixafor PET/CT seems to detect CXCR4-expressing lymphocytes at the site of infection. The hypothetical advantages of ^{68}Ga-pentixafor might lie in imaging of chronic infections in endoprostheses (no uptake in foreign-body granulomas), of osteomyelitis of the axial skeleton (which is often a pure lymphocytic infection), and of early stages of posttraumatic infection (lymphocytes are not predominant elements of bone healing).

The limitations of our study were the relatively small sample size and the retrospective setting. Further clinical and preclinical studies on ^{68}Ga-pentixafor PET/CT in skeletal infections are needed.

CONCLUSION

^{68}Ga-pentixafor PET/CT is a suitable method for imaging chronic infection of the skeleton. It might provide a diagnostic gain compared with other established methods for axial bone infections, early postoperative osteomyelitis, and periprosthetic infections, because lymphocytic infiltration can be imaged specifically.

DISCLOSURE

Saskia Kropf and Hans-Jürgen Wester are shareholders of SCINTOMICS, Germany. No other potential conflict of interest relevant to this article was reported.

REFERENCES

1. Lew DP, Waldvogel FA. Osteomyelitis. *Lancet.* 2004;364:369–379.
2. Marais L, Ferreira N, Aldous C, le Roux T. The pathophysiology of chronic osteomyelitis. *SA Orthopaedic Journal.* 2013;12:14–18.
3. Spano JP, Andre F, Morat L, et al. Chemokine receptor CXCR4 and early-stage non-small cell lung cancer: pattern of expression and correlation with outcome. *Ann Oncol.* 2004;15:613–617.
4. Spoo AC, Lubbert M, Wierda WG, Burger JA. CXCR4 is a prognostic marker in acute myelogenous leukemia. *Blood.* 2007;109:786–791.
5. Philipp-Abbrederis K, Herrmann K, Knop S, et al. In vivo molecular imaging of chemokine receptor CXCR4 expression in patients with advanced multiple myeloma. *EMBO Mol Med.* 2015;7:477–487.
6. Lapa C, Luckerath K, Kleinlein I, et al. ^{68}Ga-pentixafor-PET/CT for imaging of chemokine receptor 4 expression in glioblastoma. *Theranostics.* 2016;6:428–434.
7. Avanesov M, Karul M, Derlin T. ^{68}Ga-pentixafor PET: clinical molecular imaging of chemokine receptor CXCR4 expression in multiple myeloma. *Radiologe.* 2015;55:829–831.
8. Gourni E, Demmer O, Schottelius M, et al. PET of CXCR4 expression by a ^{68}Ga-labeled highly specific targeted contrast agent. *J Nucl Med.* 2011;52:1803–1810.
9. Wester HJ, Keller U, Schottelius M, et al. Disclosing the CXCR4 expression in lymphoproliferative diseases by targeted molecular imaging. *Theranostics.* 2015;5:618–630.
10. Demmer O, Gourni E, Schumacher U, Kessler H, Wester HJ. PET imaging of CXCR4 receptors in cancer by a new optimized ligand. *ChemMedChem.* 2011;6:1789–1791.
11. Meller B, Angerstein C, Liersch T, Ghadimi M, Sahlmann CO, Meller J. ^{68}Ga-labeled peptides for clinical trials: production according to the German Drug Act: the Gottingen experience. *Nuklearmedizin.* 2012;51:55–64.
12. Martin R, Juttler S, Muller M, Wester HJ. Cationic eluate pretreatment for automated synthesis of [^{68}Ga]CPCR4.2. *Nucl Med Biol.* 2014;41:84–89.
13. Kean LS, Sen S, Onabajo O, et al. Significant mobilization of both conventional and regulatory T cells with AMD3100. *Blood.* 2011;118:6580–6590.
14. Brave M, Farrell A, Ching Lin S, et al. FDA review summary: Mozobil in combination with granulocyte colony-stimulating factor to mobilize hematopoietic stem cells to the peripheral blood for collection and subsequent autologous transplantation. *Oncology.* 2010;78:282–288.
15. Zlotnik A, Burkhardt AM, Homey B. Homeostatic chemokine receptors and organ-specific metastasis. *Nat Rev Immunol.* 2011;11:597–606.
16. Jacobson O, Weiss ID. CXCR4 chemokine receptor overview: biology, pathology and applications in imaging and therapy. *Theranostics.* 2013;3:1–2.
17. Nanki T, Hayashida K, El-Gabalawy HS, et al. Stromal cell-derived factor-1-CXC chemokine receptor 4 interactions play a central role in CD4+ T cell accumulation in rheumatoid arthritis synovium. *J Immunol.* 2000;165:6590–6598.
18. Buckley CD, Amft N, Bradfield PF, et al. Persistent induction of the chemokine receptor CXCR4 by TGF-beta 1 on synovial T cells contributes to their accumulation within the rheumatoid synovium. *J Immunol.* 2000;165:3423–3429.
19. Brühl H, Wagner K, Kellner H, Schattenkirchner M, Schlondorff D, Mack M. Surface expression of CC- and CXC-chemokine receptors on leucocyte subsets in inflammatory joint diseases. *Clin Exp Immunol.* 2001;126:551–559.
20. Uhlén M, Fagerberg L, Hallstrom BM, et al. Proteomics: tissue-based map of the human proteome. *Science.* 2015;347:1260419.
21. Brühl H, Cohen CD, Linder S, Kretzler M, Schlondorff D, Mack M. Post-translational and cell type-specific regulation of CXCR4 expression by cytokines. *Eur J Immunol.* 2003;33:3028–3037.
22. Govaert GA, Glaudemans AW. Nuclear medicine imaging of posttraumatic osteomyelitis. *Eur J Trauma Emerg Surg.* 2016;42:397–410.
23. Meller J, Koster G, Liersch T, et al. Chronic bacterial osteomyelitis: prospective comparison of ^{18}F-FDG imaging with a dual-head coincidence camera and ^{111}In-labelled autologous leucocyte scintigraphy. *Eur J Nucl Med Mol Imaging.* 2002;29:53–60.
24. Richter WS, Ivancevic V, Meller J, et al. ^{99m}Tc-besilesomab (Scintimun) in peripheral osteomyelitis: comparison with ^{99m}Tc-labelled white blood cells. *Eur J Nucl Med Mol Imaging.* 2011;38:899–910.
25. Palestro CJ, Love C, Bhargava KK. Labeled leukocyte imaging: current status and future directions. *Q J Nucl Med Mol Imaging.* 2009;53:105–123.
26. Horger M, Eschmann SM, Pfannenberg C, et al. Added value of SPECT/CT in patients suspected of having bone infection: preliminary results. *Arch Orthop Trauma Surg.* 2007;127:211–221.
27. Bar-Shalom R, Yefremov N, Guralnik L, et al. SPECT/CT using ^{67}Ga and ^{111}In-labeled leukocyte scintigraphy for diagnosis of infection. *J Nucl Med.* 2006;47:587–594.
28. Filippi L, Schillaci O. Usefulness of hybrid SPECT/CT in ^{99m}Tc-HMPAO-labeled leukocyte scintigraphy for bone and joint infections. *J Nucl Med.* 2006;47:1908–1913.
29. Termaat MF, Raijmakers PG, Scholten HJ, Bakker FC, Patka P, Haarman HJ. The accuracy of diagnostic imaging for the assessment of chronic osteomyelitis: a systematic review and meta-analysis. *J Bone Joint Surg Am.* 2005;87:2464–2471.
30. Jamar F, Buscombe J, Chiti A, et al. EANM/SNMMI guideline for ^{18}F-FDG use in inflammation and infection. *J Nucl Med.* 2013;54:647–658.

31. Meller J, Sahlmann CO, Liersch T, Tang PH, Alavi A. Nonprosthesis orthopedic applications of ^{18}F fluoro-2-deoxy-d-glucose PET in the detection of osteomyelitis. *PET Clin.* 2006;1:107–121.
32. Guhlmann A, Brecht-Krauss D, Suger G, et al. Fluorine-18-FDG PET and technetium-99m antigranulocyte antibody scintigraphy in chronic osteomyelitis. *J Nucl Med.* 1998;39:2145–2152.
33. Zoccali C, Teori G, Salducca N. The role of FDG-PET in distinguishing between septic and aseptic loosening in hip prosthesis: a review of literature. *Int Orthop.* 2009;33:1–5.
34. Jin H, Yuan L, Li C, Kan Y, Hao R, Yang J. Diagnostic performance of FDG PET or PET/CT in prosthetic infection after arthroplasty: a meta-analysis. *Q J Nucl Med Mol Imaging.* 2014;58:85–93.
35. van der Bruggen W, Bleeker-Rovers CP, Boerman OC, Gotthardt M, Oyen WJ. PET and SPECT in osteomyelitis and prosthetic bone and joint infections: a systematic review. *Semin Nucl Med.* 2010;40:3–15.
36. Michail M, Jude E, Liaskos C, et al. The performance of serum inflammatory markers for the diagnosis and follow-up of patients with osteomyelitis. *Int J Low Extrem Wounds.* 2013;12:94–99.
37. Herrmann K, Schottelius M, Lapa C, et al. First-in-human experience of CXCR4-directed endoradiotherapy with ^{177}Lu- and ^{90}Y-labeled pentixather in advanced-stage multiple myeloma with extensive intra- and extramedullary disease. *J Nucl Med.* 2016;57:248–251.
38. Zannettino AC, Farrugia AN, Kortesidis A, et al. Elevated serum levels of stromal-derived factor-1alpha are associated with increased osteoclast activity and osteolytic bone disease in multiple myeloma patients. *Cancer Res.* 2005;65:1700–1709.
39. Bao L, Lai Y, Liu Y, et al. CXCR4 is a good survival prognostic indicator in multiple myeloma patients. *Leuk Res.* 2013;37:1083–1088.
40. Mesguich C, Zanotti-Fregonara P, Hindie E. New perspectives offered by nuclear medicine for the imaging and therapy of multiple myeloma. *Theranostics.* 2016;6:287–290.
41. Schauwecker DS. Osteomyelitis: diagnosis with In-111-labeled leukocytes. *Radiology.* 1989;171:141–146.
42. Wukich DK, Abreu SH, Callaghan JJ, et al. Diagnosis of infection by preoperative scintigraphy with indium-labeled white blood cells. *J Bone Joint Surg Am.* 1987;69:1353–1360.
43. Gratz S, Braun HG, Behr TM, et al. Photopenia in chronic vertebral osteomyelitis with technetium-99m-antigranulocyte antibody (BW 250/183). *J Nucl Med.* 1997;38:211–216.
44. Boronat-Ferrater M, Simo-Perdigo M, Cuberas-Borros G, et al. Bone scintigraphy and radiolabeled white blood cell scintigraphy for the diagnosis of mandibular osteomyelitis. *Clin Nucl Med.* 2011;36:273–276.
45. Seabold JE, Simonson TM, Weber PC, et al. Cranial osteomyelitis: diagnosis and follow-up with In-111 white blood cell and Tc-99m methylene diphosphonate bone SPECT, CT, and MR imaging. *Radiology.* 1995;196:779–788.